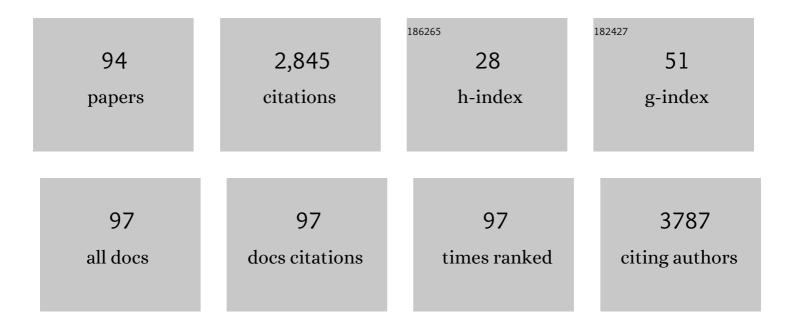
List of Publications by Year in descending order

Source: https://exaly.com/author-pdf/100284/publications.pdf Version: 2024-02-01



#	Article	IF	CITATIONS
1	Shear-strain-mediated photoluminescence manipulation in two-dimensional transition metal dichalcogenides. 2D Materials, 2022, 9, 015011.	4.4	5
2	Emergence of multiple negative differential transconductance from a WSe2 double lateral homojunction platform. Applied Surface Science, 2022, 581, 152396.	6.1	8
3	Zero power infrared sensing in 2D/3D-assembled heterogeneous graphene/In/InSe/Au. Nanoscale, 2022, 14, 3004-3012.	5.6	6
4	Parallel Alignment of Methylammonium Cations in an Orthorhombic CH ₃ NH ₃ PbCl ₃ Single Crystal Observed by Polarized Micro-Raman Scattering Spectroscopy. Chemistry of Materials, 2022, 34, 2972-2980.	6.7	3
5	Gate- versus defect-induced voltage drop and negative differential resistance in vertical graphene heterostructures. Npj Computational Materials, 2022, 8, .	8.7	8
6	Quantum hybridization negative differential resistance from non-toxic halide perovskite nanowire heterojunctions and its strain control. Nano Convergence, 2022, 9, .	12.1	6
7	Solution-processed oxide semiconductor-based artificial optoelectronic synapse array for spatiotemporal synaptic integration. Journal of Alloys and Compounds, 2021, 857, 158027.	5.5	22
8	Strain-Induced Metallization and Defect Suppression at Zipper-like Interdigitated Atomically Thin Interfaces Enabling High-Efficiency Halide Perovskite Solar Cells. ACS Nano, 2021, 15, 1805-1816.	14.6	15
9	Electronic and magnetic properties of carbide MXenes—the role of electron correlations. Materials Today Advances, 2021, 9, 100118.	5.2	35
10	Modulation of the Electronic Properties of MXene (Ti ₃ C ₂ T _{<i>x</i>}) <i>via</i> Surface-Covalent Functionalization with Diazonium. ACS Nano, 2021, 15, 1388-1396.	14.6	100
11	MXene Phase with C ₃ Structure Unit: A Family of 2D Electrides. Advanced Functional Materials, 2021, 31, 2100009.	14.9	13
12	Atomistics of Asymmetric Lateral Growth of Colloidal Zincblende CdSe Nanoplatelets. Chemistry of Materials, 2021, 33, 4813-4820.	6.7	12
13	2D Electrides: MXene Phase with C ₃ Structure Unit: A Family of 2D Electrides (Adv. Funct.) Tj ETQq1	1,0.7843 14.9	14 rgBT /C
14	An Optogeneticsâ€inspired Flexible van der Waals Optoelectronic Synapse and its Application to a Convolutional Neural Network. Advanced Materials, 2021, 33, e2102980.	21.0	65
15	Origins of genuine Ohmic van der Waals contact between indium and MoS2. Npj 2D Materials and Applications, 2021, 5, .	7.9	43
16	An Optogeneticsâ€inspired Flexible van der Waals Optoelectronic Synapse and its Application to a Convolutional Neural Network (Adv. Mater. 40/2021). Advanced Materials, 2021, 33, 2170316.	21.0	3
17	Atomistic mechanisms of seeding promoter-controlled growth of molybdenum disulphide. 2D Materials, 2020, 7, 015013.	4.4	11
18	Surface Termination-Dependent Nanotribological Properties of Single-Crystal MAPbBr ₃ Surfaces. Journal of Physical Chemistry C, 2020, 124, 1484-1491.	3.1	15

#	Article	lF	CITATIONS
19	Multi‧pace Excitation as an Alternative to the Landauer Picture for Nonequilibrium Quantum Transport. Advanced Science, 2020, 7, 2001038.	11.2	8
20	Valley depolarization in monolayer transition-metal dichalcogenides with zone-corner acoustic phonons. Nanoscale, 2020, 12, 22487-22494.	5.6	8
21	Performance Degradation in Graphene–ZnO Barristors Due to Graphene Edge Contact. ACS Applied Materials & Interfaces, 2020, 12, 28768-28774.	8.0	0
22	Raman Scattering Studies of the Structural Phase Transitions in Single-Crystalline CH ₃ NH ₃ PbCl ₃ . Journal of Physical Chemistry Letters, 2020, 11, 3773-3781.	4.6	18
23	Quasi-Fermi level splitting in nanoscale junctions from ab initio. Proceedings of the National Academy of Sciences of the United States of America, 2020, 117, 10142-10148.	7.1	14
24	First-principles-derived effective mass approximation for the improved description of quantum nanostructures. JPhys Materials, 2020, 3, 034012.	4.2	9
25	Atomic-scale view of stability and degradation of single-crystal MAPbBr ₃ surfaces. Journal of Materials Chemistry A, 2019, 7, 20760-20766.	10.3	46
26	Design and optimization of cobalt-encapsulating vertical graphene nano-hills for hydrogen evolution reaction. Journal of Materials Chemistry A, 2019, 7, 17046-17052.	10.3	11
27	All-Inkjet-Printed Vertical Heterostructure for Wafer-Scale Electronics. ACS Nano, 2019, 13, 8213-8221.	14.6	12
28	Perovskite Nanowires: Semimetallicity and Negative Differential Resistance from Hybrid Halide Perovskite Nanowires (Adv. Funct. Mater. 13/2019). Advanced Functional Materials, 2019, 29, 1970084.	14.9	1
29	Semimetallicity and Negative Differential Resistance from Hybrid Halide Perovskite Nanowires. Advanced Functional Materials, 2019, 29, 1807620.	14.9	15
30	Odd-even phonon transport effects in strained carbon atomic chains bridging graphene nanoribbon electrodes. Carbon, 2019, 142, 107-114.	10.3	9
31	Carbon Fibers: Origin and Control of Polyacrylonitrile Alignments on Carbon Nanotubes and Graphene Nanoribbons (Adv. Funct. Mater. 15/2018). Advanced Functional Materials, 2018, 28, 1870099.	14.9	2
32	Insight into the Microenvironments of the Metal–Ionic Liquid Interface during Electrochemical CO ₂ Reduction. ACS Catalysis, 2018, 8, 2420-2427.	11.2	77
33	Origin and Control of Polyacrylonitrile Alignments on Carbon Nanotubes and Graphene Nanoribbons. Advanced Functional Materials, 2018, 28, 1706970.	14.9	18
34	Data for quantum phonon transport in strained carbon atomic chains bridging graphene and graphene nanoribbon electrodes. Data in Brief, 2018, 21, 2421-2429.	1.0	0
35	HfO ₂ /HfS ₂ hybrid heterostructure fabricated <i>via</i> controllable chemical conversion of two-dimensional HfS ₂ . Nanoscale, 2018, 10, 18758-18766.	5.6	48
36	Nitrogen Doping of Carbon Nanoelectrodes for Enhanced Control of DNA Translocation Dynamics. ACS Applied Materials & Interfaces, 2018, 10, 18227-18236.	8.0	9

#	Article	IF	CITATIONS
37	Highly luminescent blue-emitting CdZnS/ZnS nanorods having electric-field-induced fluorescence switching properties. Journal of Materials Chemistry C, 2017, 5, 2098-2106.	5.5	13
38	Epitaxially Selfâ€Assembled Alkane Layers for Graphene Electronics. Advanced Materials, 2017, 29, 1603925.	21.0	24
39	Brainâ€Inspired Photonic Neuromorphic Devices using Photodynamic Amorphous Oxide Semiconductors and their Persistent Photoconductivity. Advanced Materials, 2017, 29, 1700951.	21.0	346
40	Stretching-Induced Conductance Variations as Fingerprints of Contact Configurations in Single-Molecule Junctions. Journal of the American Chemical Society, 2017, 139, 8286-8294.	13.7	29
41	First-Principles Nonequilibrium Quantum Transport Calculations and Their Applications to Next-Generation Nanoelectronic Devices. Physics and High Technology, 2017, 26, 8-14.	0.1	Ο
42	Ultrafast Discharge/Charge Rate and Robust Cycle Life for Highâ€Performance Energy Storage Using Ultrafine Nanocrystals on the Binderâ€Free Porous Graphene Foam. Advanced Functional Materials, 2016, 26, 5139-5148.	14.9	53
43	Coherent Lattice Vibrations in Mono- and Few-Layer WSe ₂ . ACS Nano, 2016, 10, 5560-5566.	14.6	62
44	Photocatalysts: Energy States of a Core-Shell Metal Oxide Photocatalyst Enabling Visible Light Absorption and Utilization in Solar-to-Fuel Conversion of Carbon Dioxide (Adv. Energy Mater. 14/2016). Advanced Energy Materials, 2016, 6, .	19.5	0
45	Theoretical Analysis and Experimental Optimization of Graphene/TMD Heterojunction Barristors. ECS Transactions, 2016, 75, 43-48.	0.5	1
46	Edge-selenated graphene nanoplatelets as durable metal-free catalysts for iodine reduction reaction in dye-sensitized solar cells. Science Advances, 2016, 2, e1501459.	10.3	88
47	Anomalous transport properties in boron and phosphorus co-doped armchair graphene nanoribbons. Nanotechnology, 2016, 27, 47LT01.	2.6	6
48	Extremely Large Gate Modulation in Vertical Graphene/WSe ₂ Heterojunction Barristor Based on a Novel Transport Mechanism. Advanced Materials, 2016, 28, 5293-5299.	21.0	92
49	Energy States of a Coreâ€Shell Metal Oxide Photocatalyst Enabling Visible Light Absorption and Utilization in Solarâ€toâ€Fuel Conversion of Carbon Dioxide. Advanced Energy Materials, 2016, 6, 1600583.	19.5	17
50	Carbon nanobuds based on carbon nanotube caps: a first-principles study. Nanoscale, 2016, 8, 2343-2349.	5.6	13
51	Recent progress in atomistic simulation of electrical current DNA sequencing. Biosensors and Bioelectronics, 2015, 69, 186-198.	10.1	48
52	Conductance recovery and spin polarization in boron and nitrogen co-doped graphene nanoribbons. Carbon, 2015, 81, 339-346.	10.3	14
53	Prediction of ultra-high ON/OFF ratio nanoelectromechanical switching from covalently-bound C60 chains. Carbon, 2014, 67, 48-57.	10.3	9
54	Distinct Mechanisms of DNA Sensing Based on Nâ€Doped Carbon Nanotubes with Enhanced Conductance and Chemical Selectivity. Small, 2014, 10, 774-781.	10.0	11

#	Article	IF	CITATIONS
55	Carbon Nanotubes: Distinct Mechanisms of DNA Sensing Based on N-Doped Carbon Nanotubes with Enhanced Conductance and Chemical Selectivity (Small 4/2014). Small, 2014, 10, 622-622.	10.0	1
56	A facile synthesis of multi metal-doped rectangular ZnO nanocrystals using a nanocrystalline metal–organic framework template. Nanoscale, 2014, 6, 10995-11001.	5.6	13
57	Atomistic mechanisms of codoping-induced p- to n-type conversion in nitrogen-doped graphene. Nanoscale, 2014, 6, 14911-14918.	5.6	30
58	Quantum interference in DNA bases probed by graphene nanoribbons. Applied Physics Letters, 2013, 103,	3.3	22
59	Boron-Vacancy Pairing and Its Effect on the Electronic Properties of Carbon Nanotubes. ECS Solid State Letters, 2012, 1, M19-M23.	1.4	2
60	Anomalous length scaling of carbon nanotube-metal contact resistance: An ab initio study. Applied Physics Letters, 2012, 100, 213113.	3.3	13
61	Intrinsically low-resistance carbon nanotube-metal contacts mediated by topological defects. MRS Communications, 2012, 2, 91-96.	1.8	9
62	First-principles Electronic Structure Calculations for Renewable Energy Research: Examples and Prospects. Physics and High Technology, 2012, 21, 9.	0.1	0
63	Conformational and conductance fluctuations in a single-molecule junction: Multiscale computational study. Physical Review B, 2010, 82, .	3.2	16
64	Electrical transport properties of nanoscale devices based on carbon nanotubes. Current Applied Physics, 2009, 9, S7-S11.	2.4	16
65	Diameter Dependence of Charge Transport across Carbon Nanotube?�Metal Contacts from First Principles. Journal of the Korean Physical Society, 2009, 55, 299-303.	0.7	3
66	Charge Transport through Polyene Self-Assembled Monolayers from Multiscale Computer Simulations. Journal of Physical Chemistry B, 2008, 112, 14888-14897.	2.6	11
67	Metal-Independent Coherent Electron Tunneling through Polymerized Fullerene Chains. Journal of Physical Chemistry C, 2008, 112, 7029-7035.	3.1	6
68	Direct and defect-assisted electron tunneling through ultrathin <mml:math xmlns:mml="http://www.w3.org/1998/Math/MathML" display="inline"><mml:mrow><mml:msub><mml:mrow><mml:mtext>SiO</mml:mtext></mml:mrow><mml:mnx from first principles. Physical Review B, 2008, 77, .</mml:mnx </mml:msub></mml:mrow></mml:math 	>2 <td>nn></td>	nn>
69	Electrical and Mechanical Switching in a Realistic [2]Rotaxane Device Model. Journal of Nanoscience and Nanotechnology, 2008, 8, 4593-4597.	0.9	8
70	Toward Numerically Accurate First-Principles Calculations of Nano-Device Charge Transport Characteristics: The Case of Alkane Single-Molecule Junctions. Journal of the Korean Physical Society, 2008, 52, 1181-1186.	0.7	9
71	First-principles study of the electrical conductance of telescopically aligned carbon nanotubes. Physical Review B, 2007, 76, .	3.2	11
72	Efficiency of Ï€â^'Ï€ Tunneling in [2]Rotaxane Molecular Electronic Switches. Journal of Physical Chemistry C, 2007, 111, 4831-4837.	3.1	23

#	Article	IF	CITATIONS
73	First-principles approach to the electron transport and applications for devices based on carbon nanotubes and ultrathin oxides. Computer Physics Communications, 2007, 177, 30-33.	7.5	4
74	First-principles study of charge transport across alkene thiolate self-assembled monolayers. , 2006, , .		0
75	Possible performance improvement in [2]catenane molecular electronic switches. Applied Physics Letters, 2006, 88, 163112.	3.3	9
76	First-principles approach to the charge-transport characteristics of monolayer molecular-electronics devices: Application to hexanedithiolate devices. Physical Review B, 2006, 73, .	3.2	60
77	Ab initio study of the effect of water adsorption on the carbon nanotube field-effect transistor. Applied Physics Letters, 2006, 89, 243110.	3.3	63
78	First-Principles Study of the Switching Mechanism of [2]Catenane Molecular Electronic Devices. Physical Review Letters, 2005, 94, 156801.	7.8	72
79	Density Functional Theory Study of the Geometry, Energetics, and Reconstruction Process of Si(111) Surfaces. Langmuir, 2005, 21, 12404-12414.	3.5	21
80	Conformations and charge transport characteristics of biphenyldithiol self-assembled-monolayer molecular electronic devices: A multiscale computational study. Journal of Chemical Physics, 2005, 122, 244703.	3.0	44
81	Structures and Properties of Self-Assembled Monolayers of Bistable [2]Rotaxanes on Au (111) Surfaces from Molecular Dynamics Simulations Validated with Experiment. Journal of the American Chemical Society, 2005, 127, 1563-1575.	13.7	202
82	Molecular Dynamics Simulation of Amphiphilic Bistable [2]Rotaxane Langmuir Monolayers at the Air/Water Interface. Journal of the American Chemical Society, 2005, 127, 14804-14816.	13.7	102
83	Density Functional Theory Studies of the [2]Rotaxane Component of the Stoddartâ^'Heath Molecular Switch. Journal of the American Chemical Society, 2004, 126, 12636-12645.	13.7	74
84	Optical excitations of Si by time-dependent density functional theory based on exact-exchange Kohn-Sham band structure. International Journal of Quantum Chemistry, 2003, 91, 257-262.	2.0	6
85	Excitonic Optical Spectrum of Semiconductors Obtained by Time-Dependent Density-Functional Theory with the Exact-Exchange Kernel. Physical Review Letters, 2002, 89, 096402.	7.8	111
86	Exact Kohn-Sham exchange kernel for insulators and its long-wavelength behavior. Physical Review B, 2002, 66, .	3.2	71
87	Electronic structure of ellipsoidally deformed quantum dots. Journal of Physics Condensed Matter, 2001, 13, 1987-1993.	1.8	11
88	Object-oriented construction of a multigrid electronic-structure code with Fortran 90. Computer Physics Communications, 2000, 131, 10-25.	7.5	6
89	Density-functional study of the hydrogen-bonded water cluster H[sub 5]O[sub 2][sup +]. AIP Conference Proceedings, 2000, , .	0.4	0
90	One-way multigrid method in electronic-structure calculations. Physical Review B, 2000, 61, 4397-4400.	3.2	32

#	Article	IF	CITATIONS
91	Two-dimensional limit of exchange-correlation energy functional approximations. Physical Review B, 2000, 61, 5202-5211.	3.2	129
92	Density-functional study of small molecules within the Krieger-Li-Iafrate approximation. Physical Review A, 1999, 60, 3633-3640.	2.5	46
93	Capacitive energies of quantum dots with hydrogenic impurity. Physical Review B, 1999, 60, 13720-13726.	3.2	15
94	Shell-filling effects and Coulomb degeneracy in planar quantum-dot structures. Physical Review B, 1997, 56, 15752-15759.	3.2	36